

INVESTIGATION OF WATER EQUIVALANCE AND SHIELDING PROPERTIES OF DIFFERENT SOLID PHANTOMS USING MCNPX CODE

H. O. TEKIN^{a,*}, M. I. SAYYED^b, T.T. ERGUZEL^c, M. KARAHAN^d,
O. KILICOGLU^e, A. MESBAHI^f, U. KARA^g

^a*Uskudar University, Vocational School of Health Services, Radiotherapy Department, Istanbul 34672, Turkey*

^b*Physics Department, University of Tabuk, Tabuk, Saudi Arabia*

^c*Uskudar University, Faculty of Engineering and Natural Sciences, Computer Engineering, Istanbul, Turkey*

^d*Uskudar University, Faculty of Engineering and Natural Sciences, Department of Bioengineering, Istanbul 34672, Turkey*

^e*Uskudar University, Vocational School of Health Services, Department of Nuclear Technology and Radiation Safety, Istanbul 34672, Turkey*

^f*Tabriz University of Medical Sciences, Medical School, Medical Physics Department, Tabriz, Iran*

^g*Suleyman Demirel University, Vocational School of Health Services, Medical Imaging Department, Isparta, Turkey*

The purpose of the present study was to evaluate the capability of Monte Carlo N-Particle Transport Code System-eXtendend (MCNPX) Monte Carlo code on investigation the water equivalent different solid phantoms and their shielding parameters and also define a standard input code in MCNPX code for future studies on related investigation field. For this purpose, we calculated the radiation mass attenuation coefficients of investigated solid phantom samples. **Materials and Methods:** To obtain the features of investigated solid phantoms, MCNPX (version 2.4.0) general purpose Monte Carlo code has been utilized for simulation studies. The material definitions of 12 different solid phantoms such as elemental mass fractions, density, geometrical shape have been done, seperately. To observe the photon transmission of selected materials, Lambert-Beer law has been utilized according to obtained output results from simulations. **Results:** The obtained values for mass attenuation coefficients of selected solid phantoms have been agreed not only with standard XCOM data but also with previous experiemental and simulation studies. Thus, our input file has been considered as a validated input for the next calculations. The results showed that, MCNPX is more consistent than FLUKA code with experiemental and standard data in the low energy region. On the other hand, the results also showed that water equivalances of some solid phantoms are quite similar with water phantom. **Conclusion:** It can be concluded that MCNPX code can be employed for solid phantom studies. It can be also concluded that, present study would be very useful for use of standard simulation geometry for medical physics and radiation dosimetry applications with solid phantoms.

(Received February 24, 2018; Accepted June 12, 2018)

Keywords: Solid Phantoms, Monte Carlo Simulation, MCNPX

1. Introduction

In recent years, solid phantom materials have been frequently used for dosimetry studies and calibration of radiation detectors in nuclear medicine, radiotherapy and radiology applications. On the other hand, tissue-equivalent materilas have been utilized to investigate doses received by patients [1-3]. In previous dosimetry studies, water is recommended as a reference material environment for absorbed dose calculations [4-5]. There are some situations that make it necessary

*Corresponding uthor: huseyinozan.tekin@uskudar.edu.tr

to use solid water phantoms such as water permeability of radiation detectors [6]. The basic properties expected from a solid phantom have the closest similar properties to water. Those physical properties can be defined as total radiation mass attenuation coefficient (μ/ρ), mass energy absorption coefficient (μ_{en}/ρ) [7] effective atomic number, relative electron density, material density, similar absorption of radiation [8]. Due to the varying energy values depending on the field of use such as therapy or diagnostic, the dominant interaction pattern may also change. Therefore, Compton effect can be considered as more dominant interaction in high energy regions such as radiation therapy applications. In addition, the photoelectric effect also can be considered more dominant in low energy region such as brachytherapy and x-ray applications [9]. One can say that solid phantom materials have application-based usage in medical area. Therefore, scientific studies on this subject are made experimentally. However, simulation technique for investigation of radiation interaction is found radiologically safer, less time consuming, cost effective and applicable for desired energy of radiation. It is found that Monte Carlo simulation is suitable method for investigation of radiation interaction with materials in various literature elsewhere [10-13]. However, MCNPX simulation in many different types of solid phantom materials and determination of their shielding parameters such as mass attenuation coefficients are not found in literature. This has encouraged us to investigate for water equivalency of various solid phantom materials using MCNPX simulation code by considering various attenuation and shielding parameters.

The results presented by Hill showed that RMI457 Solid Water, PW and RW3 had transmission values that were in most cases within 1.0% of those of water thus meeting the ICRU requirements for water equivalency [9]. The results presented by Mihailescu showed that PMMA and solid water WT1 solid phantom can be converted to appropriate depth in water by means of depth-scaling [14]. The results presented by Demir showed that RMI-457, plastic water and RW solid phantoms can be used for radiation dosimetry of photons in the energy range from 59.5 to 1332.5 keV [15]. The results presented by Park showed that polystyrene which is one of the most common material in good agreement and could be used to confirm the feasibility of the solid phantom as a substitute for water for high energy photon beam [16]. In this study, we used gamma ray transmission calculations and obtained the shielding parameters of investigated solid phantom materials. The following solid phantom materials PWDT, Polystyrene, RW3, PAGAT, VW, PMMA, PW, RMI-457, A-150, PERSPEX, PRESAGE were investigated by using MCNPX (version 2.4.0) general purpose Monte Carlo code for water equivalency.

In present study, the obtained results have been compared with available published data by various authors. In present investigation, PWDT, Polystyrene, RW3, PAGAT, VW, PMMA, PW, RMI-457, A-150, PERSPEX, PRESAGE solid phantom materials were evaluated for water equivalency. The elemental mass fractions of the investigated solid phantom materials are given in Table 1 [9-17]. The calculated results were compared with both the measured results and the published data.

2. Materials and methods

2.1. Radiation shielding parameters

In theory, nearly all the materials can be used for shielding of radiation if they employed in a specific material thickness. However, the attenuation features of those materials are dependent upon the density of the shielding material. One can say that a dense shielding material with a higher atomic number has a better shielding properties for energetic gamma rays. For monochromatic gamma beams, the intensity reduces as the photon beam propagates through the shielding material according to the Lambert-Beer law by following equation [1].

$$[I=I_0 \exp (-\mu t)] \quad (1)$$

In this formula, where I_0 is the incident intensity, t is the path length, and μ is the sample's linear attenuation coefficient. This coefficient depends on the elemental or composition chemical of the sample.

2.2. Mass attenuation coefficients

The linear attenuation coefficient depends on the density. Due to this reason, a data which is independent of the density (μ/ρ) of the substance is needed. This information, which is independent from density is called the mass attenuation coefficient and its unit is m^2/kg . The term of mass attenuation coefficient (μ/ρ) is the one of the important value to evaluate the shielding properties of shielding materials and can be calculated. The mass attenuation coefficient can be obtained by dividing the linear attenuation coefficient (μ) by density (ρ) of investigated shielding material. On the other hand, the mass attenuation coefficient (μ/ρ) of a shielding material sample at a specific energy is the sum of the products of the weight fraction and the mass attenuation coefficient of the element i at that energy namely:

$$\mu/\rho = \sum_i w_i(\mu/\rho)_i$$

where w_i and $(\mu/\rho)_i$ are the fractional weight and the total mass attenuation coefficient of the i th constituent in the mixture shielding material sample.

2.3. MCNPX simulation code

Monte Carlo N-Particle Transport Code System-extended (MCNPX) version 2.4.0 (Los Alamos national lab, USA) general purpose Monte Carlo code was applied for determination of mass attenuation coefficients of investigated solid phantom materials. MCNPX is a Monte Carlo code for simulation of various physical interactions at large energy range. MCNPX is fully three-dimensional and it utilizes extended nuclear cross section libraries and uses physics models for particle types [18]. MCNPX operates extended nuclear cross section libraries and uses specific physics models for different type of particles.

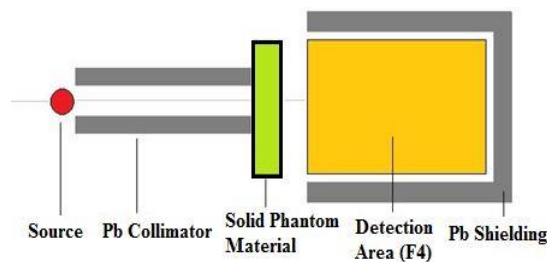


Fig. 1. MCNPX total simulation geometry for calculations of mass attenuation coefficients.

This code is a major and powerful code for photon attenuation and energy deposition studies. Similar to the methodology in this study, some MCNPX studies for different radiation applications were found in the literature [19-29]. In present investigation, each simulation parameters such as cell specifications, surface specifications, material specifications and position determinations of each simulation tools have been defined in input file according to their physical features. In present investigation, gamma ray sources with various energies have been defined as a point isotropic source. The source has been defined in the mode card of MCNPX input file as a point source at photon energies of 59.5 keV, 80.9 keV, 140.5 keV, 356.5 keV, 661.6 keV, 1173.2 keV, 1332.5 keV, respectively. The total simulation geometry of present investigation for mass attenuation coefficient calculations can be seen in Fig.1. To investigate the mass attenuation coefficient, geometry and material composition of solid phantom material has been defined in input file. As it can be seen from Fig.1, solid phantom material has been located as an attenuator sample between source and detection area. A point isotropic radiation source was also placed at a

point before the solid phantom material. To obtain the absorbed dose amount in the detection field, average flux tally F4 has been used. This type of tally in MCNPX scores average flux in a point or cell. In addition, 10^8 particles have been tracked as the number of particle (NPS variable). MCNPX calculations were done by using Intel® Core™ i7 CPU 2.80 GHz computer hardware.

2.4. WinXcom program

In present investigation, WinXcom program [30] was also used to calculate the gamma ray mass attenuation coefficients of the investigated glass samples. WinXcom program is a user friendly calculation program and input parameter specifications are quite flexible and easy to access. In the WinXcom program, each solid phantom material were defined by their elemental fractions which also given in Table 1. Afterwards, the well-known gamma ray energies such as 59.5 keV, 80.9 keV, 140.5 keV, 356.5 keV, 661.6 keV, 1173.2 keV, 1332.5 keV have been defined. The attenuation coefficients of the selected glasses were finally calculated by the WinXcom program.

2.5. Statistical reliability index – pearson correlation coefficient (R)

Pearson correlation (R) is a straightforward approach to evaluate the relationship between two variables that measures how well multiple variables move together and fit in a linear fashion. Pearson correlation is being widely employed in recent studies focusing on pattern recognition, medical data, mathematical modelling and decision analysis studies. Supposing the variables x and y existing in a dataset, the following equation as given in equation 3 defines the population correlation coefficient (ρ):

$$\rho = \frac{\sigma_{x,y}}{\sigma_x \sigma_y} = \frac{\text{Cov}(x,y)}{\sigma_x \sigma_y} \quad (3)$$

Here, the more positive ρ value means the more positive population correlation while the more negative ρ identifying the more negative association. If the population correlation coefficient, ρ , is close to 1 it points a high positive linear relation between two independent variables while a negative ρ is indicating a negative relation between the variables. Apart from the aforementioned cases, a ρ with a value close to 0 points shows little linear association for the variables. In order to obtain the correlation coefficient, both σ_x^2 and σ_y^2 values, the covariance of x and y are also calculated. On the other hand, since the parameters of a population are generally either unknown or difficult to collect all data, an alternative approach using r_{xy} is employed from the sample dataset in order to estimate the unknown population parameter.

The following expression given in equation 4 identifies the correlation coefficient of the sample that is being used to converge the population parameter.

$$r_{xy} = \frac{\sum_{i=1}^n (x_i - \bar{x})(y_i - \bar{y})}{\sqrt{\sum_{i=1}^n (x_i - \bar{x})^2} \sqrt{\sum_{i=1}^n (y_i - \bar{y})^2}} \quad (4)$$

Where x_i and y_i are the i^{th} pair observation value, $i=1,2,3\dots n$. \bar{x} and \bar{y} are sample means for x and y variables respectively. Another parameter generated from R value is known as the coefficient of determination (R^2) is a measure used to assess how well a model explains and predicts the outcome. R^2 is considered as an indicative marker explaining the variability in the outcome caused by the change in the input variables. The coefficient of determination, commonly known as "R-squared," is used as a guideline to measure the accuracy of the model.

3. Results

The mass attenuation coefficients (μ/ρ) of the investigated phantom materials for different gamma rays (59.5, 80.9, 140.5, 356.5, 661.6, 1173.2 and 1332.5 keV) calculated by MCNPX code and XCOM software are tabulated in Table 2-13. In addition, the MCNPX and XCOM results for RMI-457 (as an example) are shown in Fig. 2. From Table 2 and Fig. 2 it can be noted that the

values of μ/ρ calculated based on the MCNPX code are in a very good agreement with those obtained theoretically by XCOM. Fig.3-5 shows the variation of μ/ρ for each sample along with the water as a function of energy. From Fig. 3 (a-d) it can be seen that the μ/ρ for RMI-457 and RW-3 phantoms are in close agreement to that of water.

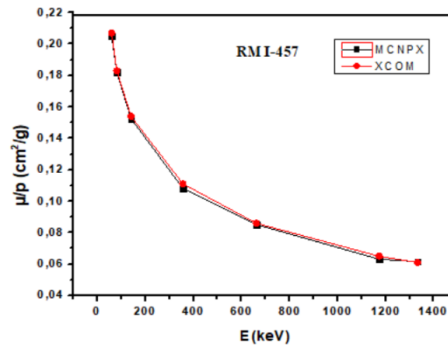


Fig. 2. Comparison of MCNPX and standard XCOM data.

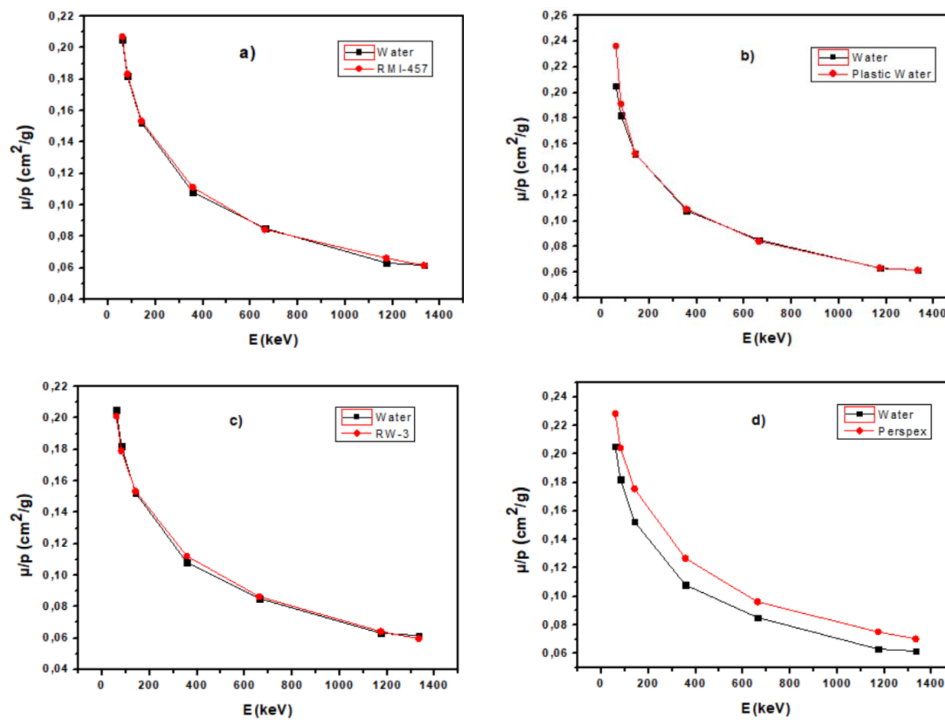


Fig. 3. A comparison of measured mass attenuation coefficients of different solid phantoms (a) RMI-457, (b) Plastic Water, (c) RW-3, (d) Perspex for water equivalency.

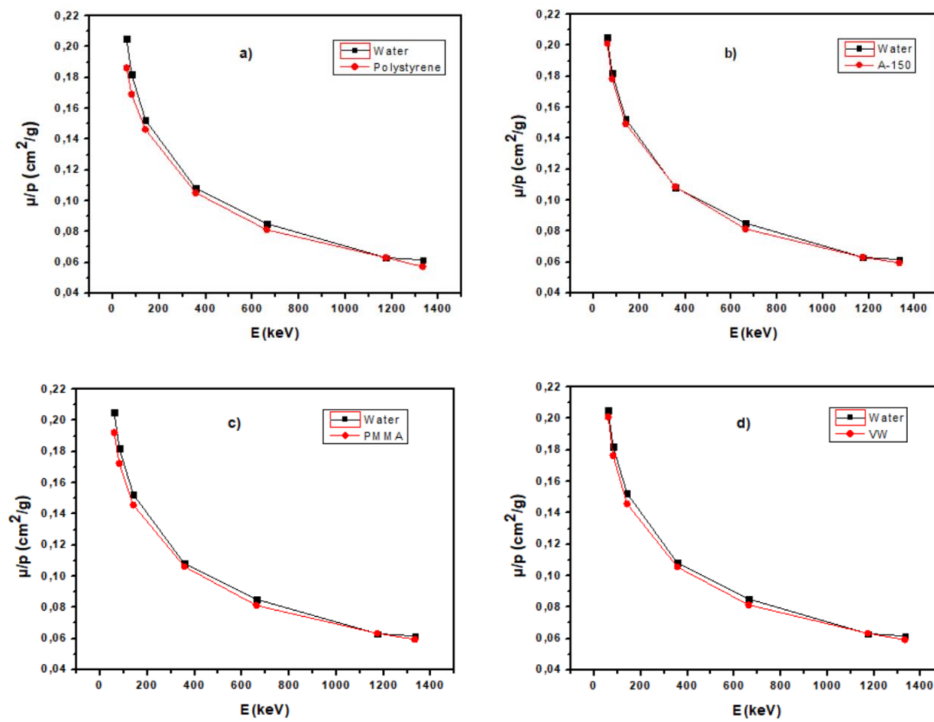


Fig. 4. A comparison of measured mass attenuation coefficients of different solid phantoms (a) Polystyrene, (b) A-150, (c) PMMA, (d) VW for water equivalency.

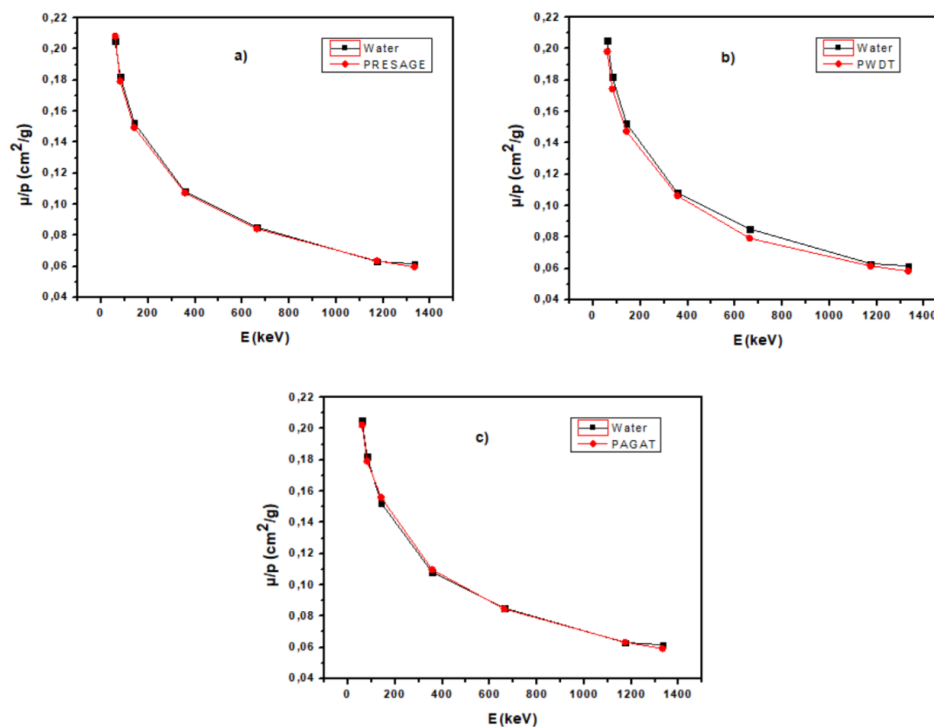


Fig. 5. A comparison of measured mass attenuation coefficients of different solid phantoms (a) Presage, (b) PWDT, (c) PAGAT for water equivalency

The deviation in the μ/p with respect to water for RMI-457 and RW-3 samples lies within the range 0-4.9% and 0.65-3.79% respectively. In addition, the largest differences in the μ/p values with respect to water are recorded for perspex, polystyrene and PWDT.

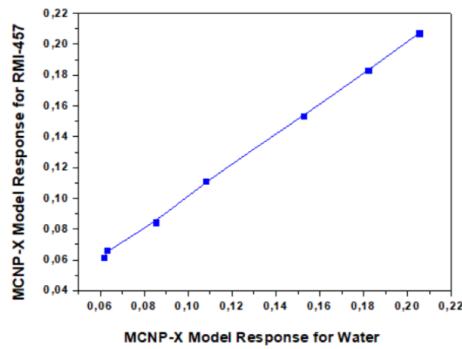


Fig.6. Regression line of MCNP-X model response for the phantom RMI-457 and water

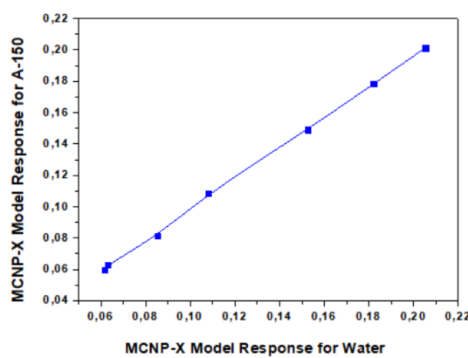


Fig. 7. Regression line of MCNP-X model response for the phantom A-150 and water.

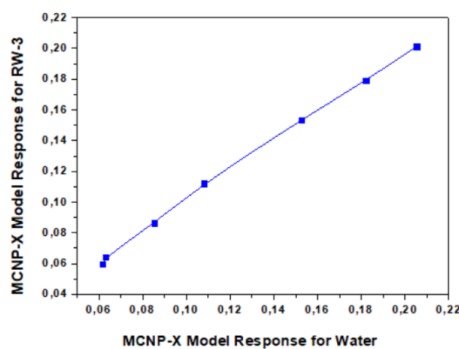


Fig. 8. Regression line of MCNP-X model response for the phantom PAGAT and water.

The μ/ρ values for Perspex are high than those for water, while the μ/ρ values for polystyrene and PWDT are lower than those for water. The μ/ρ results showed that maximum differences between the μ/ρ for Perspex, polystyrene and PWDT phantoms with respect to water are 19% at 1173.2 keV, 9.25% at 59.5 keV and 7.04% at 661.6 keV respectively. Fig. 6, Fig. 7, and Fig. 8 are used to plot the regression line In order to demonstrate the similarity between the phantom's and pure water response to the MCNP-X model.

Table 1. The elemental mass fractions of investigated solid phantom materials.

Element	Polystyrene	RW3	PWDT	VW	PAGAT	PMMA	PW	RMI-457	A-150	PERSPEX	PRESAGE	Water
H	0.0774	0.0759	0.074	0.077	0.1059	0.0805	0.0925	0.0809	0.1013	0.0805	0.0892	0.1119
B	0	0	0.0226	0	0	0	0	0	0	0	0	0
C	0.9226	0.9041	0.467	0.6874	0.0681	0.5998	0.6282	0.6722	0.7755	0.5998	0.6074	0
N	0	0	0.0156	0.0227	0.0242	0	0.01	0.024	0.0351	0	0.0446	0
O	0	0.008	0.3352	0.1886	0.8008	0.3196	0.1794	0.1984	0.0523	0.3996	0.2172	0.8881
F	0	0	0	0	0	0	0	0	0.0174	0	0	0
Mg	0	0	0.0688	0	0	0	0	0	0	0	0	0
Al	0	0	0.014	0	0	0	0	0	0	0	0	0
P	0	0	0	0	0.0002	0	0	0	0	0	0	0
Cl	0	0	0	0.0013	0.0002	0	0.0096	0.0013	0	0	0.0334	0
Ca	0	0	0	0.0231	0	0	0.0795	0.0232	0.0184	0	0	0
Ti	0	0.012	0		0	0	0	0	0	0	0	0
Br	0	0	0	0	0	0	0.0003	0	0	0	0.0084	0

Table 2. Mass attenuation coefficients for Water.

Energy (keV)	Water (density=1.00 g/cm ³)				
	MCNPX	FLUKA	XCOM	Measured	EGSnc
59.5	0.205	0.193	0.207		
80.9	0.182	0.174	0.183		
140.5	0.152	0.145	0.154	0.148	0.151
356.5	0.108	0.108	0.111		
661.6	0.085	0.083	0.086		
1173.2	0.063	0.065	0.065		
1332.5	0.061	0.059	0.061		

Table 3. Mass attenuation coefficients for RMI-457.

Energy (keV)	RMI-457 (density=1.030 g/cm ³)				
	MCNPX	FLUKA	XCOM	Measured	EGSnc
59.5	0.207	0.196	0.209		
80.9	0.183	0.176	0.184		
140.5	0.153	0.146	0.154	0.151	0.151
356.5	0.111	0.109	0.112		
661.6	0.084	0.083	0.086		
1173.2	0.066	0.065	0.066		
1332.5	0.061	0.06	0.061		

Table 4. Mass attenuation coefficients for Plastic Water.

Energy (keV)	Plastic Water (density=1.013 g/cm ³)				
	MCNPX	FLUKA	XCOM	Measured	EGSnc
59.5	0.236	0.229	0.239		
80.9	0.191	0.186	0.195		
140.5	0.152	0.15	0.156	0.151	0.152
356.5	0.109	0.108	0.111		
661.6	0.084	0.083	0.086		
1173.2	0.063	0.064	0.065		
1332.5	0.061	0.06	0.061		

Table 5. Mass attenuation coefficients for RW-3.

Energy (keV)	RW-3 (density=1.050 g/cm-3)				
	MCNPX	FLUKA	XCOM	Measured	EGSnrc
59.5	0.201	0.191	0.204		
80.9	0.179	0.172	0.182		
140.5	0.153	0.146	0.155	0.149	0.153
356.5	0.112	0.11	0.113		
661.6	0.086	0.084	0.087		
1173.2	0.064	0.065	0.066		
1332.5	0.059	0.061	0.062		

Table 6. Mass attenuation coefficients for Perspex.

Energy (keV)	Perspex (density=1.190 g/cm-3)				
	MCNPX (This study)	FLUKA	XCOM	Measured	EGSnrc
59.5	0.228	0.218	0.23		
80.9	0.204	0.195	0.207		
140.5	0.175	0.168	0.177	0.166	0.17
356.5	0.126	0.125	0.128		
661.6	0.096	0.096	0.099		
1173.2	0.075	0.074	0.075		
1332.5	0.07	0.068	0.07		

Table 7. Mass attenuation coefficients for Polystyrene.

Energy (keV)	Polystyrene (density=1.060 g/cm-3)				
	MCNPX (This study)	FLUKA	XCOM	Measured	EGSnrc
59.5	0.186		0.187		
80.9	0.169		0.171		
140.5	0.146		0.147		
356.5	0.105		0.107		
661.6	0.081		0.083		
1173.2	0.063		0.063		
1332.5	0.057		0.059		

Table 8. Mass attenuation coefficients for A-150.

Energy (keV)	A-150 (density=1.127 g/cm-3)				
	MCNPX (This study)	FLUKA	XCOM	Measured	EGSnrc
59.5	0.201		0.201		
80.9	0.178		0.179		
140.5	0.149		0.151		
356.5	0.108		0.109		
661.6	0.081		0.084		
1173.2	0.063		0.064		
1332.5	0.059		0.06		

Table 9. Mass attenuation coefficients for PMMA.

Energy (keV)	PMMA (density=1.127 g/cm-3)				
	MCNPX (This study)	FLUKA	XCOM	Measured	EGSnrc
59.5	0.192		0.193		
80.9	0.172		0.174		
140.5	0.145		0.148		
356.5	0.106		0.107		
661.6	0.081		0.083		
1173.2	0.063		0.063		
1332.5	0.059		0.059		

Table 10. Mass attenuation coefficients for VW.

Energy (keV)	VW (density=1.030 g/cm-3)				
	MCNPX (This study)	FLUKA	XCOM	Measured	EGSnrC
59.5	0.201		0.202		
80.9	0.176		0.177		
140.5	0.145		0.148		
356.5	0.105		0.107		
661.6	0.081		0.083		
1173.2	0.063		0.063		
1332.5	0.059		0.059		

Table 11. Mass attenuation coefficients for PRESAGE.

Energy (keV)	PRESAGE (density=1.101 g/cm-3)				
	MCNPX (This study)	FLUKA	XCOM	Measured	EGSnrC
59.5	0.208		0.21		
80.9	0.179		0.182		
140.5	0.149		0.151		
356.5	0.107		0.108		
661.6	0.084		0.084		
1173.2	0.063		0.064		
1332.5	0.059		0.059		

Table 12. Mass attenuation coefficients for PWDT.

Energy (keV)	PWDT (density=1.039 g/cm-3)				
	MCNPX (This study)	FLUKA	XCOM	Measured	EGSnrC
59.5	0.198		0.199		
80.9	0.174		0.176		
140.5	1.147		1.148		
356.5	0.106		0.107		
661.6	0.079		0.082		
1173.2	0.061		0.062		
1332.5	0.058		0.058		

Table 13. Mass attenuation coefficients for PAGAT.

Energy (keV)	PAGAT (density=1.026 g/cm-3)				
	MCNPX (This study)	FLUKA	XCOM	Measured	EGSnrC
59.5	0.202		0.204		
80.9	0.179		0.181		
140.5	0.15		0.152		
356.5	0.109		0.11		
661.6	0.084		0.085		
1173.2	0.063		0.064		
1332.5	0.059		0.06		

Table 14. Mass Attenuation Coefficient Correlations of MCNP-X and FLUKA Models with XCOM.

Phantom Material	Modelling Approach		
	MCNPX	FLUKA	XCOM
Water (d=1g/cm3)	0.999868	0.999678	1.000000
RMI-457 (d=1.03g/cm3)	0.999935	0.999785	1.000000
Plastic water (d=1.013g/cm3)	0.999905	0.999962	1.000000
RW-3 (d=1.05g/cm3)	0.999894	0.999854	1.000000
Perspex (d=1.19g/cm3)	0.999879	0.999827	1.000000
Polystyrene (d=1.06g/cm3)	0.999886	-	1.000000
A-150 (d=1.127g/cm3)	0.999881	-	1.000000
PMMA (d=1.127g/cm3)	0.999846	-	1.000000
VW (d=1.03g/cm3)	0.999826	-	1.000000
Presage (d=1.101g/cm3)	0.999950	-	1.000000
PWDT (d=1.039g/cm3)	1.000000	-	1.000000
PAGAT (d=1.026g/cm3)	0.999993	-	1.000000

Table 15. Mass Attenuation Coefficient Correlations of Phantom Materials and Water for MCNP-X Model.

Phantom Material	Water
	MCNP-X
RMI-457 (d=1,03g/cm ³)	0,99968
Plastic water (d=1,013g/cm ³)	0,99390
RW-3 (d=1,05g/cm ³)	0,99910
Perspex (d=1,19g/cm ³)	0,99937
Polystyrene (d=1,06g/cm ³)	0,99854
A-150 (d=1,127g/cm ³)	0,99968
PMMA (d=1,127g/cm ³)	0,99965
VW (d=1,03g/cm ³)	0,99956
Presage (d=1,101g/cm ³)	0,99939
PWDT (d=1,039g/cm ³)	0,99962
PAGAT (d=1,026g/cm ³)	0,99980

4. Discussion

The coefficient of determination value of three phantoms versus pure water validates that the mass attenuation coefficients are quite similar. The correlation of the models with XCOM data as given in table 14 results that the predictive ability of MCNPX is relatively better compared to FLUKA model studied by Demir et al.,(2017). In addition to model performance comparison process, the response of solid material phantoms was also studied. Here, as given in table 15, the correlation of the phantoms was calculated in order to underline the convergence of the solid phantom materials to pure water. From this discussion, we can conclude that since Perspex, polystyrene and PWDT phantoms possess μ/ρ values that significantly differ from those of water, thus these phantoms do not match the water and tissue equivalency requirements, while RMI-457, A-150 and PAGAT samples are the most water equivalent phantoms according to μ/ρ values.

5. Conclusions

In present investigation, MCNPX code (version 2.4.0) has been utilized for the calculations of mass attenuation of investigated solid phantom materials such as PWDT, Polystyrene, RW3, PAGAT, VW, PMMA, PW, RMI-457, A-150, PERSPEX, PRESAGE. Moreover, the mass attenuation coefficients of investigated solid phantom materials have been compared for water equivalency. It is obvious from our findings that RMI-457 and RW-3 solid phantoms have similar properties with water and can be used for radiation dosimetry in the investigated energy range. On the other hand, it can be concluded that MCNPX Monte Carlo code has more consistent results with standard XCOM data. The results underline that the output of MCNPX model outperforms FLUKA in terms of mass attenuation coefficient prediction capability. The correlation of both MCNPX and FLUKA models are quite competitive. Besides, with the use of various phantoms a comparative performance evaluation process was performed. The results point out that RMI-457, A-150 and PAGAT are quite similar in terms of mass attenuation capability, as reported previously Demir et al. (15) and Hill et al. (17).

References

- [1] A. K. Jones, D. E. Hintenlang, W. E. Bolch, Med. Phys. **30**, 2072 (2003).
- [2] R. Kienböck, Arch. Roentgen Ray **11**, 17 (1906). R. A. Jucius, G. X. Kambic, Radiation dosimetry in computed dosimetry, Appl.

- [3] Opt. Instrum. Eng. Med. **127**, 286 (1977).
- [4] IAEA, IAEA TRS-277, 1987.
- [5] IAEA, IAEA TRS-398, 2000.
- [6] G. Mitchell, T. Kron, M. Back, Phys. Med. Biol. **43**, 1343 (1998).
- [7] C. C. Ferreira, R. E. M. Ximenes Filho, J. W. Vieira, A. Toma, M. E. Poletti, C. A. B. Garcia, A. F. Maia, Nuclear Instruments and Methods in Physics Research B **268**, 2515 (2010).
- [8] P. Andreo, D. T. Burns, K. Hohlfield, M. S. Huq, T. Kanai, F. Laitano, V. Smyth, S. Vynckier, Technical Report Series No. 398, International Atomic Energy Agency, Vienna 2000.
- [9] R. F. Hill, S. Brown, C. Baldock, Radiation Measurements **43**, 1258 (2008).
- [10] N. Demir, U. A. Tarim, M.-A. Popovici, Z. N. Demirci, O. Gurler, I. Akkurt, Journal of Radioanalytical and Nuclear Chemistry **298**(2), 1303 (2013).
- [11] Huseyin Ozan Tekin, Science and Technology of Nuclear Installations **2016**, Article ID 6547318, 7pages.
- [12] A. Jehouani, R. Ichaoui, M. Boulkheir, Applied Radiation and Isotopes **53**(4-5), 887 (2000).
- [13] Y. Chul-Young, H. Suck-Ho, Applied Radiation and Isotopes **70**, 2133 (2012).
- [14] D. Mihailescu, C. Borcia, Romanian Reports in Physics **58**(4), 415 (2006).
- [15] N. Demir, U. Akar Tarim, O. Gurler, Int. J. Radiat. Res. **15**(1), 123 (2017).
- [16] D-W. Park, J-K. Lee, Journal of the Korean Physical Society **69**, (4).
- [17] R. Hill, Z. Kuncic, C. Baldock, Med. Phys. **37**, 4355 (2010).
- [18] RSICC Computer Code Collection. 2002. MCNPX User's Manual Version 2.4.0. Monte Carlo N-Particle Transport Code System for Multiple and High Energy Applications.
- [19] H. O. Tekin, Science and Technology of Nuclear Installations. Volume **2016**, Article ID 6547318.
- [20] I. Akkurt, H. O. Tekin, A. Mesbahi, Acta Physica Polonica A **128** (2-B): 332 (2015).
- [21] H. O. Tekin, U. Kara, Journal of Communication and Computer (13), 32 (2016).
- [22] H. O. Tekin, V. P. Singh, U. Kara, T. Manici, E. E. Altunsoy, CBU Journal of Science **12**(2) (2016).
- [23] H. O. Tekin, V. P. Singh, T. Manici, Journal of Polytechnic **19**(4), 617 (2016).
- [24] H. O. Tekin, V. P. Singh, T. Manici, Applied Radiation and Isotopes, 2016.
- [25] H. O. Tekin, T. Manici, Nuclear Science and Techniques **28**, 95 (2017).
- [26] H. O. Tekin, V. P. Singh, E. E. Altunsoy, T. Manici, M. I. Sayyed, Iranian Journal of Medical.
- [27] M. I. Sayyed, M. Y. Al-Zaatreh, M. G. Dong, M. H. M. Zaid, K. A. Matori, H. O. Tekin, <https://doi.org/10.1016/j.rinp.2017.07.028>
- [28] M. G. Dong, R. El-Mallawany, M. I. Sayyed, H. O. Tekin, Radiation Physics and Chemistry **141**, 172 (2017)–178.
- [29] H. O. Tekin, V. P. Singh, T. Manici, E. E. Altunsoy, Journal of Radiation Protection and Research **42**(3), 1 (2017).
- [30] L. Gerward, N. Guilbert, K. B. Jensen, H. Levring, Radiat. Phys. Chem. **71**(3), 653 (2004).